Organic Process Research & Development

ARTICLE

pubs.acs.org/OPRD

The Development of a Robust Process for a CRF_1 Receptor Antagonist

Sévrine Broxer,* Monica A. Fitzgerald, Chris Sfouggatakis, Jessica L. Defreese, Evan Barlow, Gerald L. Powers, Michael Peddicord, Bao-Ning Su, Yue Tai-Yuen, Charles Pathirana, and James P. Sherbine

Process Research and Development, Bristol-Myers Squibb Company P.O. Box 191, New Brunswick, New Jersey 08903, United States

ABSTRACT: A scalable and robust process was developed for the preparation of pexacerfont (**2**), a pyrazolotriazine corticotropin-releasing factor receptor 1 antagonist (CRF_1). The formation of the core hydroxypyrazolotriazine moiety was achieved through two consecutive cyclizations of a semicarbazide, employing reaction conditions that are significantly milder than those reported in the literature. Further conversion to the key chloropyrazolotriazine intermediate was accomplished through a novel catalytic process using phosphorous oxychloride as the chlorinating agent. The active pharmaceutical ingredient **2** was obtained in >99.5% purity with a 68% overall yield for the six synthetic steps.

INTRODUCTION

Corticotropin-releasing factor (CRF) is a 41 amino acid peptide[1] that plays a critical role in the body's response to stress.[2] Hypersecretion of CRF from the hypothalamus is proposed to trigger depression and anxiety-related disorders.[3] While two receptors have been identified, CRF binds preferentially to the CRF_1 receptor. A significant amount of research has been invested in developing a CRF_1 receptor antagonist, as studies suggest that blocking the CRF_1 receptor could treat the diseases that result from elevated CRF levels. Accordingly, a variety of small-molecule CRF_1 receptor antagonists, containing the pyrazolo[1,5-*a*]-1,3,5-triazine structural motif as in **1** (Figure 1), have been studied as therapeutic agents for the treatment of various CRF-related disorders.[4a,4b] The Discovery Chemistry group within Bristol-Myers Squibb focused on the syntheses and structure−activity relationships of 8-(4-methoxyaryl)pyrazolo[1,5-*a*]-1,3,5-triazine CRF_1 receptor antagonists as potential anxiolytic drugs. Their efforts led to the identification of compound **2** for advancement into clinical development as a potent CRF_1 antagonist (Figure 1).[5]

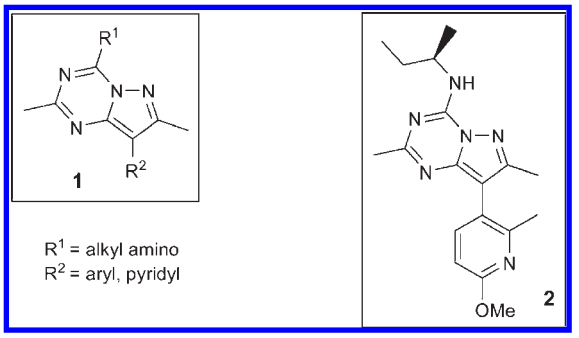

Figure 1

The synthetic strategy employed by Discovery Chemistry for the preparation of clinical candidate **2** is outlined in Scheme 1.[4−6] A key feature to the synthesis involved a Pd-mediated coupling of 6-methoxy-3-bromo-2-methyl pyridine **3**[7] with 4-iodo-4-methyl-isoxazole **5**,[8] followed by isomerization under basic conditions to provide β-ketonitrile **7** as the sodium enolate form.[9] Treatment of **7** with excess hydrazine monohydrate in refluxing toluene afforded aminopyrazole **8** in 76% yield over the two steps from oxazole **6**. Amidine **9** was next generated via condensation of amine **8** with ethyl acetimidate in the presence of 1 equiv of glacial acetic acid. Subsequent treatment with diethyl carbonate in the presence of sodium ethoxide in refluxing ethanol formed pyrazolotriazinone **10** in 79% yield for the two steps. Chlorination was then achieved with 4 equiv of phosphorus oxychloride in the presence of Hunig's base in toluene at reflux to generate the key chloropyrazolotriazine intermediate **11**. Finally, coupling of intermediate **11** with (*R*)-2-butylamine provided the final product **2** in ∼50% yield over the two steps.

While this sequence satisfied the initial material requirements and was amenable to the preparation of analogs, its use for kilogram-scale preparation of **2** presented a number of challenges. First, the synthesis was lengthy, requiring eight isolations from the bromopyridyl starting material **3** and relied on extensive use of column chromatography for both impurity removal and isolation of noncrystalline intermediates. A primary goal for process development was to eliminate the use of chromatography and define process conditions (henceforth referred to as telescope procedures) that allowed crude noncrystalline or unstable intermediates to be directly used in the next transformation. Telescoped processes also provide additional efficiencies in that they minimize the number of isolation steps. Second, the use of large quantities of highly toxic and dangerously unstable hydrazine[10] posed a serious challenge from a safety perspective. As such, an alternative synthesis of aminopyrazole **8** would be required for multikilogram-scale production. Finally, the penultimate chloropyrazolotriazine intermediate **11** was found to be highly unstable and readily hydrolyzed when exposed to moisture. Measures to address these stability considerations would be key aspects for the design of the final-step chemistry and process.

A retrosynthetic analysis of **2** maintains the late-stage installation of the chiral amine moiety, as described in the discovery synthesis, leading to the known hydroxypyrazolotriazine intermediate **10**[5] (Scheme 2). A disconnection strategy that relied on an alternative cyclization at the six-position of the triazine core was then considered.

Received: October 7, 2010
Published: January 31, 2011

Scheme 1

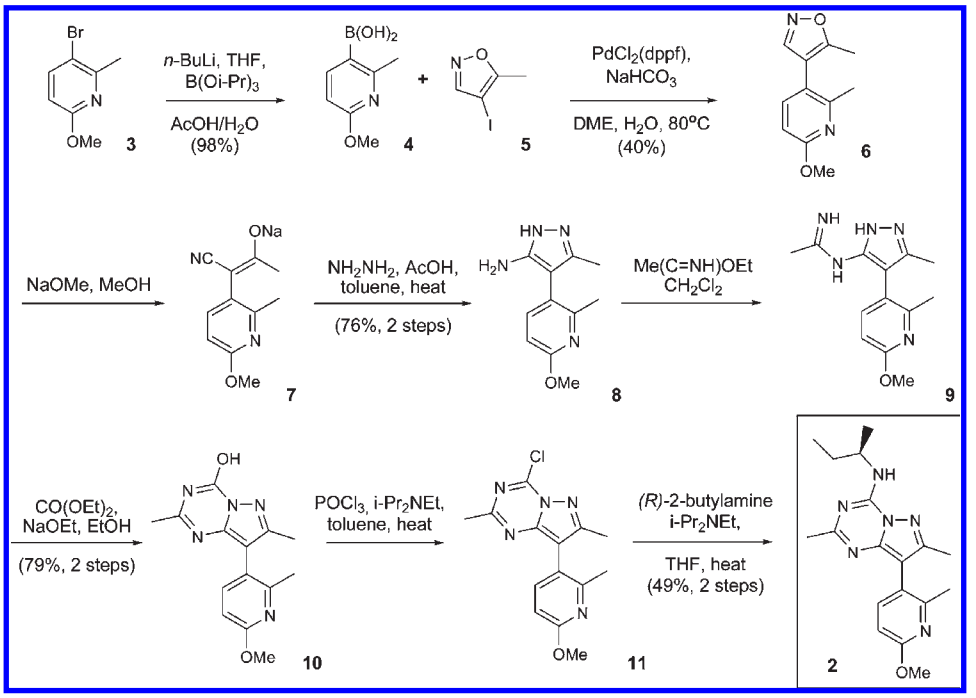

In the forward sense, this transformation was envisioned to proceed via condensation of an orthoester derivative with aminopyrazole **12** bearing the carboxamide functionality. Further disconnection of the pyrazole reveals semicarbazone **13** which can be assembled by condensation of the known cyanoketone **14** and commercially available semicarbazide **15**. This revised synthetic strategy allows for a more convergent synthesis in which hydrazine can be replaced with the less toxic semicarbazide reagent.

RESULTS AND DISCUSSION

Synthesis of Semicarbazone 13. The point of departure for the modified process route from the Discovery Chemistry route begins at the pyridyl acetonitrile **16**.[11] The modified process route utilized an alternative method to generate enolate derivate **7** based on condensation of **16** with ethyl acetate.[12] This transformation was readily achieved under basic conditions using potassium *tert*-butoxide in THF to provide a mixture of *cis*- and *trans*-enolates **17** (Scheme 3). Following neutralization and concentration via distillation, the potassium enolate **17** was then treated with an aqueous solution of semicarbazide hydrochloride salt **15** in the presence of 2-propanol[13] to promote crystallization of **13** directly from the reaction media, albeit as a mixture of the *trans* and semicarbazone isomers.[14] The process was successfully scaled to >50 kg to provide high-quality **13** in 96% yield as a 80:20 mixture in favor of semicarbazone **13b**,[15] however, a number of challenges remained from an analytical perspective.

Scheme 2

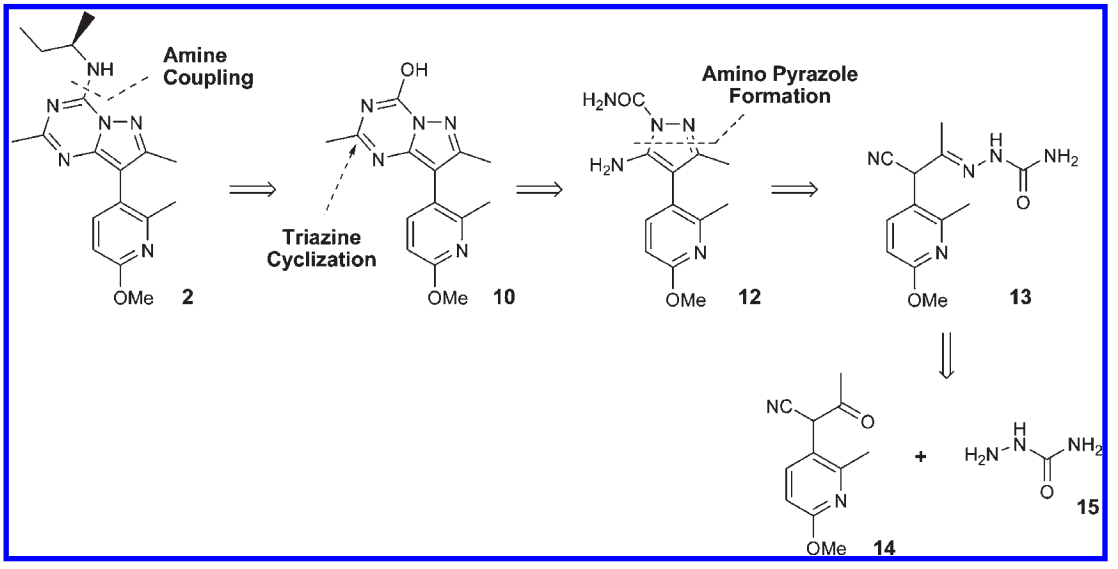

dx.doi.org/10.1021/op100270u |*Org. Process Res. Dev.* 2011, 15, 343–352

Scheme 3

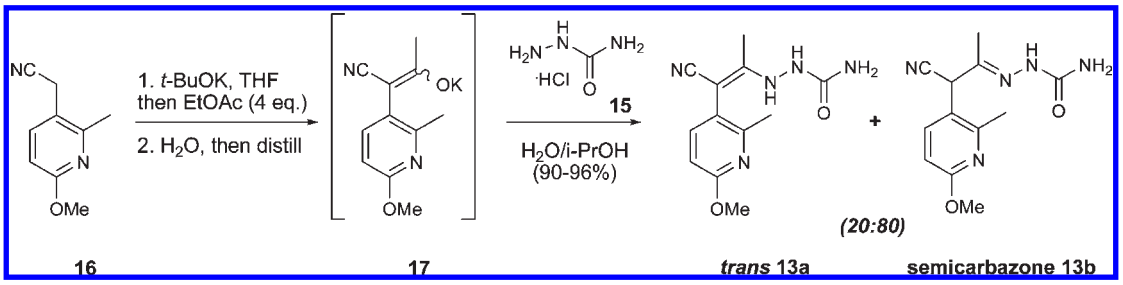

The major challenge encountered in the preparation of **13**, was the ability to reliably analyze the isomeric product mixture. Isomers **13** exhibited poor solubility in most common organic solvents. For the purposes of HPLC analyses, the isomers were dissolved in DMSO/MeCN with sonication in order to facilitate full dissolution. Once in solution, however, the isomers rapidly interconverted, resulting in inconsistencies from assay to assay. The sonication step also caused the formation of the cyclized intermediate **12**, as well as related impurity **8** (Scheme 4). Due to these challenges, an indirect purity assay was developed based on derivitization. Treatment of **13** with a solution of 0.01 wt % triethylamine (TEA) in acetonitrile resulted in full conversion to **12** along with trace quantities of **8** as a minor byproduct. To accurately calculate the purity, a response factor for **12** and the relative response factor (RRF) of **12** to **8** were measured. The chemical purity of **13** could then be estimated by summing the area of impurity **8**, weighted by the RRF, to the area of **12**.

Given that a conventional method to determine the purity for **13** was not directly available, stringent quality criteria were established for starting material **16** and the subsequent penultimate hydroxypyrazolotriazine intermediate **10**. This bracketing approach to the analytical testing ensured we could achieve the requisite purity for **10** even if the absolute purity for **13a** and **13b** could not be ascertained. Furthermore, penultimate hydroxypyrazolotriazine **10** is a robust crystalline substance that provides excellent impurity removal. Thus, **10** was selected as a quality gate-keeper intermediate for the synthesis.

Scheme 4

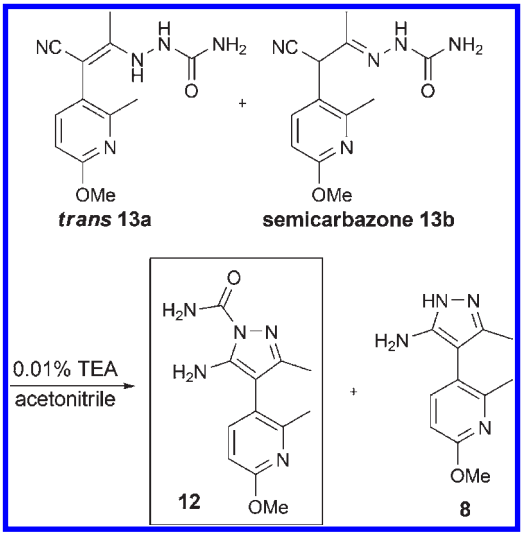

Synthesis of Hydroxypyrazolotriazine 10. The analytical challenges to measure the overall purity for the isomeric mixture **13** did not impact the downstream chemistry as both readily cyclized to pyrazole **12** in the presence of 20 mol % DBU (1,8-diazabicyclo[5.4.0]undec-7-ene) in acetonitrile at 0 °C (Scheme 5). The subsequent addition of 25 mol % *p*-TsOH (*p*-toluenesulfonic acid) and 1.3 equiv of TMOA (trimethylorthoacetate) led to imidate **18** which smoothly cyclized to form triazine **10** within 3−5 h at reflux. The reaction workup made use of the acidic nature of **10**, since when dissolved into an aqueous sodium hydroxide solution, the non acidic impurities selectively partitioned to the toluene wash layer. Isolation was then accomplished by citric acid addition to regenerate the conjugate acid, which directly crystallized. Following filtration and drying, the product was isolated as the monohydrate form in 66−70% yield and high purity (99.7 AP).

While the process for **10** was suitable for use in initial scale-up (implemented on a 10 kg input scale), there was a potential for the product to crystallize directly from the reaction mixture. This strategy would serve to both eliminate the cumbersome acid−base workup and allow isolation of **10** as an anhydrous form.[16,17] A screen of reaction parameters revealed that the process could tolerate a wide range of concentrations (5−15 L/kg) and reagent charges (1−20 mol % DBU; 1.5 − 25 mol % *p*-TsOH). The latitude of reagent stoichiometry allowed for a reduction in the base (5 mol %) and acid (8 mol %) catalyst loadings, which when combined with the use of toluene as the solvent during the workup, induced the spontaneous crystallization of **10** directly from the reaction mixture. Consequently, the aqueous workup was eliminated and high quality anhydrous hydroxypyrazolotriazine **10** was isolated in 75−80% yield on laboratory scale.

Implementation of this process on a 55 kg scale in the pilot plant afforded hydroxypyrazolotriazine **10** in 71% isolated yield, which was comparable to laboratory scale. However, the amount of **10** remaining in the mother liquors was greater than expected (16% yield loss). Further examination of reaction conditions indicated that the solubility of **10** in toluene was dramatically increased by increasing DBU levels.[18] Accordingly, a simple way to optimize the recovery of **10** was to reduce the amount of DBU further to 1 mol %.

Understanding the reaction mechanism and decomposition pathways further aided the process development and optimization. The first reaction consists of isomers **13a** and **13b** cyclizing to form a single intermediate **12** within 1 h at ambient temperature. Extended reaction times resulted in partial urea cleavage to

dx.doi.org/10.1021/op100270u |*Org. Process Res. Dev.* 2011, 15, 343–352

Scheme 5

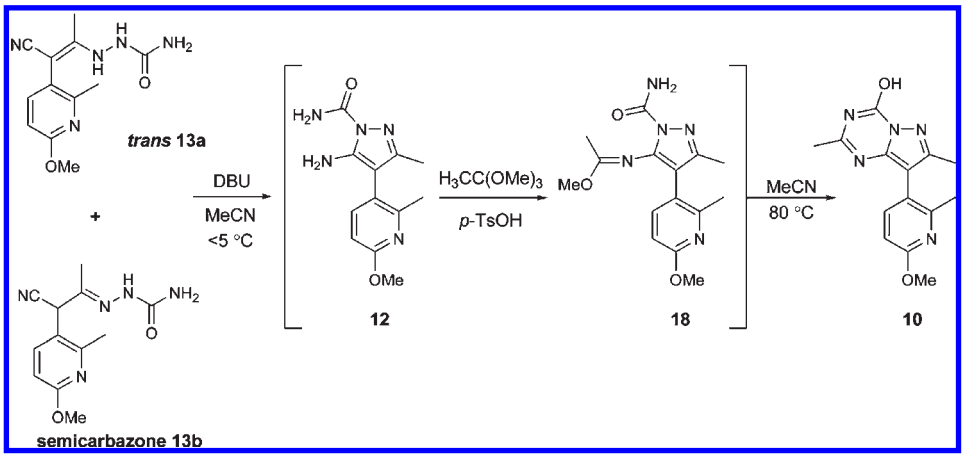

pyrazole **8** (Scheme 4). This was solved by a reduction in operating temperature to <5 °C, which controlled impurity **8** to acceptable levels (<0.5%) within a 2 h reaction time frame. Following the addition of *p*-TsOH and TMOA, the corresponding imidate **18** (Scheme 5) was observed as the major species within 30 min at reflux. Heating the reaction mixture at reflux for an additional 3 h resulted in complete conversion to cyclized product **10**.

During the conversion of **12** to **10**, approximately 10% of a transient species was observed within 1−2 h, but had entirely disappeared after 3 h. LCMS analysis revealed that the unknown compound had the same mass as imidate **18**, suggesting the possibility of an acyl group migration. To confirm this hypothesis, an isolated sample of pyrazole **12** was heated to 100 °C in toluene, resulting in a 90:10 mixture of **12** and the unknown compound which was subsequently identified as acyl migration product **19** by NMR analyses (Scheme 6). Similarly, heating a sample of isolated isomer **19** produced the same equilibrium 90:10 mixture.

We surmised that under the reaction conditions (*p*-TsOH/TMOA), isomer **19** generated the corresponding imidate **20** (Scheme 7), as suggested by LCMS analysis. By analogy, one would expect a similar equilibrium to exist between **20** and **18** as between **12** and **19**. As intermediate **18** can efficiently close to afford **10**, imidate **20** remains a productive intermediate for the formation of **10**.

The use of *p*-TsOH as catalyst was not optimal, owing to its reaction with the methanol generated during the conversion of **12** to **10** to produce the corresponding genotoxic *p*-toluene sulfonate methyl ester.[19] Although the *p*-TsOH methyl ester was formed in low levels in **10** (<150 ppm), it was effectively removed during crystallization and could not be detected in the final product **2**. Nevertheless, we preferred to use an alternative acid to avoid this concern. Several acids (HCO_2H, AcOH, HCl, TFA) were screened to determine if they were suitable replacements for *p*-TsOH. TFA was selected as the replacement because it provided an improved reaction profile with respect to acyl migration and des-acyl impurities **19** and **8**, and its corresponding methyl ester derivative is a nongenotoxic impurity.

Although the performance of TFA as a catalyst was superior to *p*-TsOH, the issue of the overall low yield remained. This was attributed, in part, to an unproductive side-product, imidate **21**, which forms upon cleavage of the amide moiety (Scheme 8). This impurity formed via two distinct pathways. In the first, the amide group is initially cleaved to afford **8** and subsequent TMOA/TFA addition formed **21** (pathway **a**, Scheme 8). The

Scheme 6

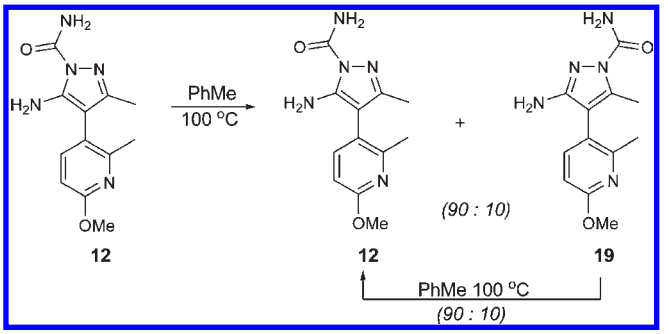

formation of **8** could be minimized by charging the DBU at low temperature (<5 °C) under anhydrous conditions (KF <600 ppm). Alternatively, cleavage of intermediate **18** (pathway **b**) could also form **21**. This pathway was avoided by using a substoichiometric amount of TFA (20 mol %) and charging TMOA at 0 °C.

Several large-scale laboratory reactions (100−650 g) were performed to test the optimized reaction conditions described above. The product losses to the mother liquor were reduced to 4% with a corresponding higher isolated yield of 86% (vs 71%) and a purity of 99.7 AP.

While the first-generation process addressed concerns regarding the *trans* and semicarbazone isomers (**13a** and **13b**), and provided high-quality penultimate hyroxypyrazolotriazine **10**, a more efficient and robust process was required for further scale-up. This goal was realized through the course of development work by understanding the reaction pathway, impurity formation, and material losses. By eliminating the acid/base workup, reducing reagent charges, and identifying TFA as a replacement for *p*-TsOH, an efficient multikilogram-scale process for the preparation of anhydrous **10** was developed. More importantly, the yield and cycle time improvements did not compromise quality, and the high level of purity was maintained while eliminating the potential

dx.doi.org/10.1021/op100270u |*Org. Process Res. Dev.* 2011, 15, 343–352

Scheme 7

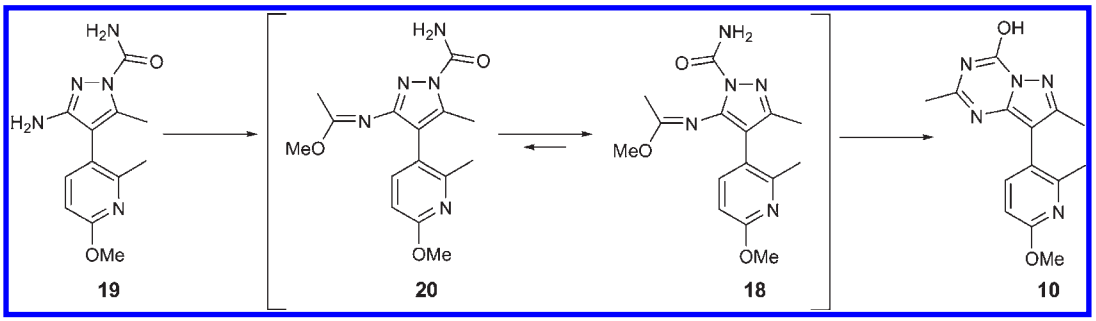

Scheme 8

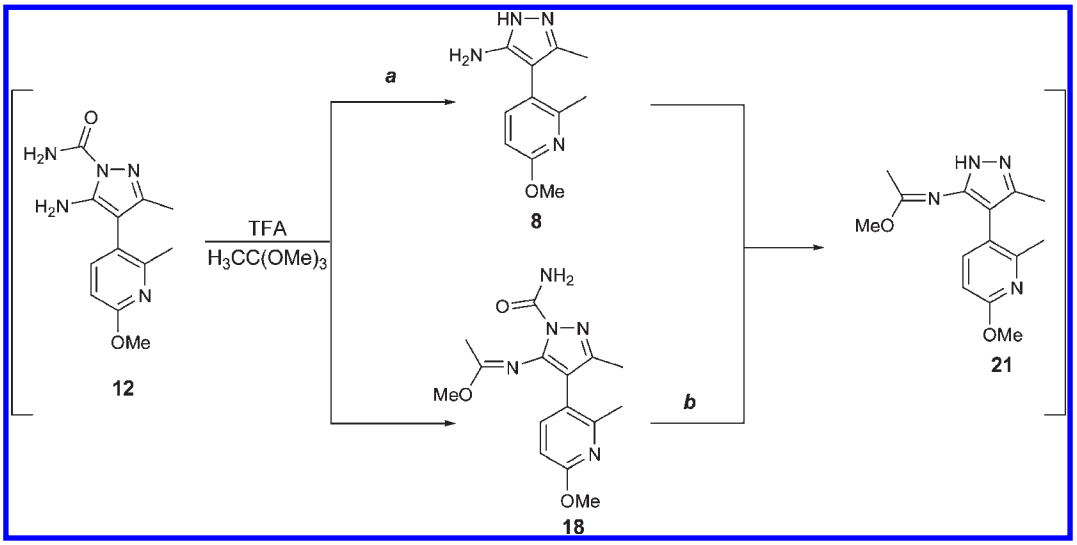

for a genotoxic impurity (GTI) as demonstrated from the process comparisons shown in Table 1.

Optimizing the API Step: Evolution of the Base-Catalyzed Chlorination. The final transformation in the synthesis was to append the (*R*)-2-butylamine side chain. This is most efficiently accomplished by electrophilic activation of the core via conversion of the hydroxyl group to the chloride, followed by nucleophilic displacement with the amine. Chlorinations of hydroxypyridine systems such as compound **10** are well established in the literature and are often performed using neat refluxing $POCl_3$.[20] However, reactions using these conditions present a significant scale-up challenge from both a safety and environmental standpoint. We sought to accomplish the chlorination of compound **10** under milder conditions.

Table 1. Hydroxypyrazolotriazine (10) process comparison

	first generation	second generation	third generation
acid cat.	*p*-TsOH (0.2 equiv)	*p*-TsOH (0.08 equiv)	TFA (0.2 equiv)
base cat.	DBU (0.2 equiv)	DBU (0.05 equiv)	DBU (0.01 equiv)
extractions	3	0	0
titrations	2	0	0
distillations	1	1	1
isolated form	monohydrate	anhydrous	anhydrous
yield (%)	68	71	86
HPLC (AP)	99.7	99.7	99.7
potential GTI	yes	yes	no

Our initial approach to **2** through chlorination of hydroxypyrazolotriazine **10** involved heating a solution of **10** in toluene with diisopropylethylamine (DIPEA), $POCl_3$ and benzyltributylammonium chloride (BTAC)[21] at 80 °C.[22] The BTAC provides a chloride ion source which has been shown to increase the rate of reaction.[23] Once the chlorination was complete, 1.7 equiv of (*R*)-2-butylamine and 1 equiv of DIPEA were added to furnish **2** in 42−57% yield (entry 1, Table 2).

The process posed several challenges during the initial scale-up investigations. The presence of the stoichiometric amount of BTAC resulted in a biphasic reaction mixture that made scalability, mixing, and sampling unreliable. The reaction workup in this case furnished a red, oily solution that required filtration through silica gel for color removal. Additionally, as **2** is very soluble in toluene (370 mg/mL), a lengthy solvent exchange to octane was required to achieve the desired solvent composition for crystallization.

dx.doi.org/10.1021/op100270u |*Org. Process Res. Dev.* 2011, 15, 343–352

Table 2. Reaction conditions examined for chlorination of 10[a]

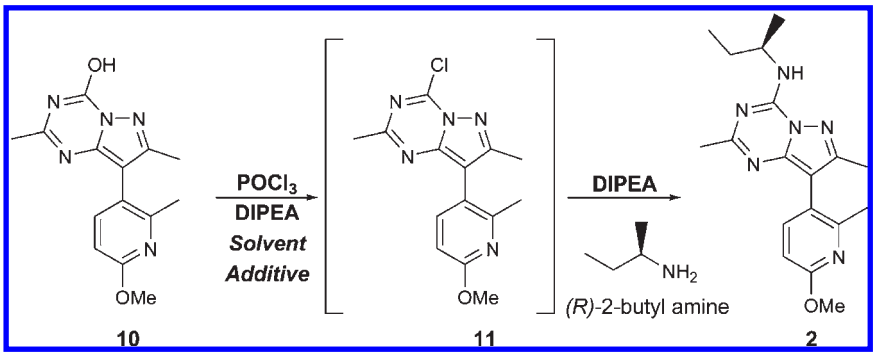

entry	solvent	additive	temperature (°C)	time (h)[b]	yield (%)[c]
1	toluene	0.1 equiv BTAC	70−75	2−4	42−57
2	toluene/MeCN	0.6 equiv BTAC	70−75	2−4	59−70
3	MeCN	none	70−75	1	62
4	MeCN	0.01 equiv DABCO	20	1	78
5	MeCN	none	20	48	90[d]

[a] 1.3 equiv of $POCl_3$, 2.0 equiv of DIPEA; 1.0 equiv of DIPEA, 1.7 equiv of (*R*)-2-butylamine. [b] Determined as >98% conversion to **11** by HPLC analysis. [c] Based on isolated **2**. [d] Conversion to **11**.

From a quality perspective, the presence of a dimeric impurity, formed during the course of the chlorination, proved challenging as well. On the basis of LC/MS data and literature precedent,[24] we anticipated the formation of the symmetric dimer **22** (Figure 2), however, single-crystal X-ray analysis revealed it was the regioisomeric dimer **23**.[25] This dimeric impurity was observed at levels greater than 1% based on HPLC area, and could not be purged to acceptable levels by recrystallization of **2**.

Although the initial strategy was to qualify **23** to a level of 1.0 AP in toxicological studies, we continued to study methods to further lower its level and streamline the process. Reducing the amount of BTAC to 0.6 equiv and adding 0.6 volumes of MeCN resulted in a homogeneous solution that allowed for representative in-process sampling and provided a yield improvement of approximately 15% (entry 2, Table 2). Subsequently, it was found that BTAC was not critical for the chlorination step if performed in MeCN as solvent (entry 3, Table 2).[26] Increasing the volume of MeCN compared to the toluene process (15 vs 8 L/kg) also reduced the amount of **23** by 50%. In addition, the solubility profile of **2** in MeCN allowed for isolation of the final product directly from the reaction mixture by crystallization from MeCN/H_2O.

Earlier work on previous CRF drug candidates revealed that DABCO (1,4-diazabicyclo[2.2.2]octane) could be used as a catalyst to accelerate the chlorination reaction.[27] Toward this end, we were pleased to find that the presence of 1 mol % of DABCO afforded complete conversion to chloropyrazolotriazine **11** within 1 h at 20 °C (entry 4, Table 2), and further reduced byproduct **23** to 0.2 AP. By comparison, the reaction in MeCN in the absence of DABCO required 48 h to reach 90% conversion (entry 5, Table 2). This highlights the powerful catalytic properties of DABCO for the chlorination.[28]

To enable process optimization, additional impurities were characterized in an effort to gain a deeper understanding of the reaction profile and to improve the overall quality of the final product. The DABCO-catalyzed chlorination gave rise to ≤0.5% of a new impurity identified as the chloro-derivative **24** (Scheme 9). Since this impurity is a potential alkylating agent, its level required close monitoring in the final product. We hypothesized that the formation of **24** was the result of nucleophilic attack of DABCO on the proposed O-phosphorylated intermediate **25**. Presumably, chloride ion displacement of DABCO (pathway **a**) provides the desired product **11**. Conversely, attack at either of the three α-carbons of the activated DABCO intermediate **26** (pathway **b**) would produce impurity **24**.

The dealkylation of tertiary amines during chlorinations of compounds such as **10** with $POCl_3$ is known,[29] as was the opening of DABCO ammonium salts by chloride.[30] As such, we focused our attention toward identification of an alternate catalyst that would mitigate the formation of an impurity that has the potential to act as an alkylating agent. A brief summary of the tertiary amines surveyed is shown in Table 3. The acyclic and less sterically strained tertiary amines such as triethyl- and triphenylamine (entries 1 and 2), as well as pyridine and *N*-methylpyrrolidine (entries 3 and 4), were less active than DABCO in catalyzing the chlorination. Comparable conversions to **11** were observed

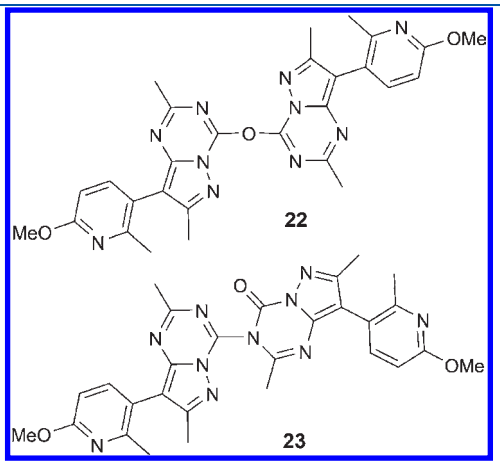

Figure 2

dx.doi.org/10.1021/op100270u |*Org. Process Res. Dev.* 2011, 15, 343–352

Scheme 9

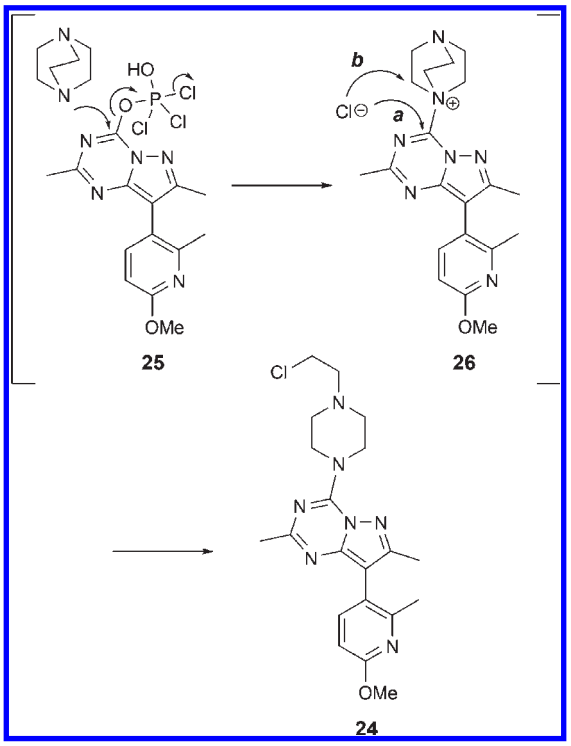

when amines that were structurally similar to DABCO were used (entries 5 and 6); however, in order to avoid chlorinated impurities, these amines were not pursued.

Table 3. Examples of tertiary amine catalysts used in chlorination of 10

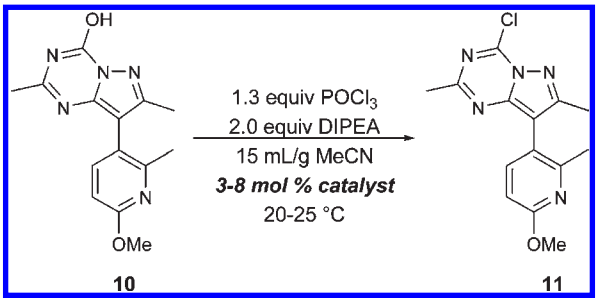

entry	amine	Time (h)	Conv. (%)
1	Triethylamine	21	93
2	Triphenylamine	21	92
3	Pyridine	21	88
4	*N*-Methylpyrrolidine	24	98
5	Quinuclidine	1	95
6	3-Quinuclidinol	1.5	98
7	*N*-Methylmorpholine	0.2	98
8	*N*-Ethylmorpholine	28	94
9	Morpholine	8	90
10	*N*-Methylpiperidine	2	98
11	1,4-dimethylpiperazine	1	98

The reaction promoted with 6 mol % *N*-methylmorpholine (NMM) resulted in complete conversion to **11** within 12 min (entry 7, Table 3), whereas other derivatives of morpholine were less efficient (entries 8 and 9). While other saturated six-membered heterocyclic amines were effective catalysts (entries 10 and 11), we selected NMM due to its higher catalytic activity .

The stoichiometry of NMM was optimized at 0.5 mol % which led to >98% conversion to **11** within 1 h at 25 °C, although the dealkylated impurity **27** (Figure 3) still formed in analogy to the DABCO catalyzed reaction. The decrease in catalyst loading reduced the formation of the dealkylated impurity **27**, which forms at levels proportional to the amount of catalyst used. Importantly, a chlorinated impurity analogous to **24** was not observed in the NMM-catalyzed process since any undesired chloride ion attack would presumably occur on the primary methyl group of NMM to form trace amounts of chloromethane gas.

In addition to the dimer and catalyst-related impurities, four impurities related to DIPEA incorporation were identified (**28**−**31**, Figure 4). Dealkylated DIPEA impurities **28** and **29**, observed during the chlorination step, are thought to form either by elimination or by attack of chloride ion on either the isopropyl or ethyl groups of a DIPEA-activated intermediate analogous to **26** (Scheme 9). The formation of both impurities was minimized below 0.15% by a rapid addition of $POCl_3$.[31]

Following the chlorination, compound **11** was telescoped into the amine displacement reaction via in situ treatment with (*R*)-2-butylamine and an additional stoichiometric equivalent of DIPEA to effect the transformation to the final product **2**. The displacement of the chloride occurs readily at −5 °C, but is also accompanied by the formation of two additional DIPEA-related impurities (**30**−**31**, Figure 4) that were observed on scale. Enamine impurity **30** and C-bound adduct **31** were envisioned to form through the iminium salt of DIPEA.[32,33] The enamine tautomer can displace the chloride ion in **11** to form impurity **30**. Alternatively, the initial iminium ion could be trapped by nucleophilic addition of **11** to form **31**. Although levels of **30** were as high as 1% during the reaction, it was completely purged during the isolation. Unfortunately, impurity **31** was formed in variable amounts (0.1 − 0.5%) during the reaction and did not purge during the crystallization. While rapid addition of (*R*)-2-butylamine minimizes its formation, such a practice was not feasible on scale given the exothermic nature of the addition (T_{ad} = 64 °C). Reversing the order of amine additions ((*R*)-2-butylamine followed by DIPEA) effectively controlled the formation of **31** to below detection. All of these impurities were effectively controlled by either the order or rate of addition of reagents and by the workup conditions.

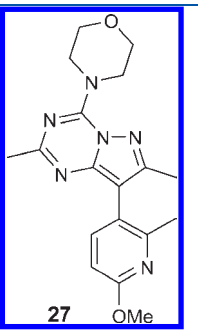

Figure 3

dx.doi.org/10.1021/op100270u |*Org. Process Res. Dev.* 2011, 15, 343–352

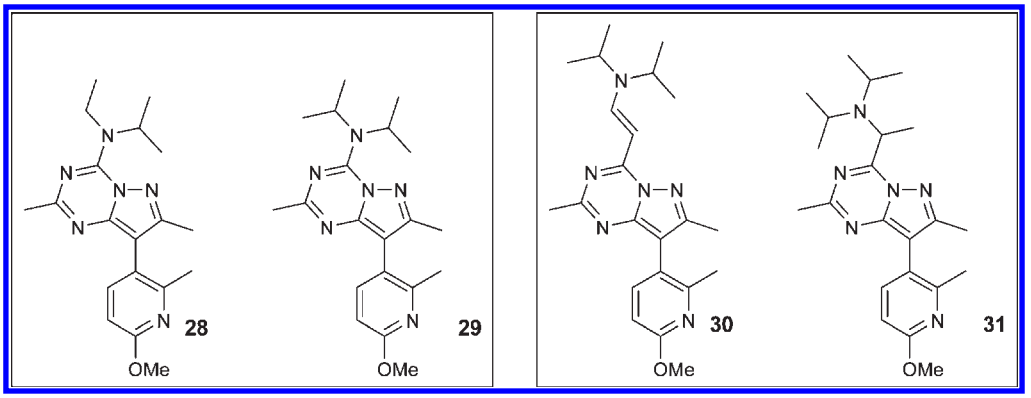

Figure 4. DIPEA-related impurities.

Early iterations of the process required multiple crystallizations of the final product to meet the required purity specifications, whereas the process improvements described above dramatically improved the product quality and yield, without the need for a recrystallization (Table 4).

Furthermore, the optimizations to the reaction portion of the process allowed for a simplification of the reaction workup in the telescoped preparation of **2**. The final optimized process used aqueous NaOH to quench the excess phosphorous chloride, followed by heating to 65 °C to dissolve the resulting slurry. The solution was then cooled and diluted with water to induce crystallization, and the product was isolated by filtration. The two-step chlorination/amination sequence, provided high-quality drug substance **2** in a 82% yield (>99.8 AP, 99.2 wt %, and 99.8% chiral purity) on greater than 40 kg scale.

Table 4. API (2) Process Comparison

	BTAC process	DABCO Process	NMM (final) process
chlorination temp	80 °C	20−25 °C	20−25 °C
extractions	3	3	0
distillations	1	1	0
polish filtration	yes (silica gel)	no	no
final solvent system	toluene/ octane	acetonitrile/ water	acetonitrile/ water
Yield (crude)	63%	78%	82%
HPLC AP (crude)	>98.85	>97.93	>99.8
recrystallization	yes	yes	no
yield (recrys)	81%	81%	N/A
overall yield	53%	61%	82%

CONCLUSION

A robust and scalable process was developed for the synthesis of **2**. The key challenges addressed were an understanding of the complex reaction sequence in the synthesis of hydroxypyrazolotriazine **10**, the development of a high-yielding and more environmentally friendly process for the chlorination step, and the characterization and origin of impurities found in the final drug substance. A significant improvement in cycle time, yield, and quality were achieved at each stage of development, resulting in a process that can be safely and reproducibly run on scale. With the improvements described, an efficient and commercially viable synthesis of CRF candidate **2** was achieved in six steps (three isolations) with an overall yield of 68% (Scheme 10).

EXPERIMENTAL SECTION

The experimental outlined below provide representative procedures for what was run on scale in the kilo/pilot plant facilities. Reagents and solvents were acquired from a variety of sources and employed without further purification. ^{1}H NMR spectra were obtained at 400 MHz, ^{13}C NMR spectra were obtained at 100 MHz at 25 °C in $CDCl_3$ except as indicated. Chemical shifts are reported in ppm downfield from an internal tetramethylsilane standard or relative to the residual solvent signal. Coupling constants (J) are given in hertz. Moisture determinations were performed with a Karl Fischer titrator. HPLC analyses were performed using a reverse phase technique. Infrared spectra were recorded in an FT instrument at 4.00 cm^{-1} resolution.

2-(4-Methoxy-2-methyl-3-pyridyl)-3-methylbut-2-enylnitrile Semicarbazide (13a) and 2-(4-Methoxy-2-methyl-3-pyridyl)-3-oxobutyronitrile Semicarbazone (13b). To an anhydrous solution of ethyl acetate (169 L) and tetrahydrofuran (242 L) (KF <600 ppm), was added **16** (69.9 kg, 432 mol), followed by a solution of potassium *tert*-butoxide (303 L, 496 mol, 1.0 M in tetrahydrofuran). The reaction mixture was heated to 45 °C, and HPLC analysis indicated >98% conversion to enolate **17** within 30 min. The addition of H_2O (105 L) was followed by vacuum distillation at an average rate of 260 L/h. The jacket temperature was gradually increased to 65 °C, and the reaction mixture temperature remained below 25 °C during the vacuum distillation. Once ~400 L remained, the jacket temperature was decreased to 25 °C, and isopropyl alcohol (140 L) was charged followed by a solution of semicarbazide hydrochloride salt (96.3 kg, 863 mol) in water (385 L). The reaction was held for 4 h at 35 °C at which time HPLC analysis indicated >99% conversion to the isomeric mixture **13**. The product crystallized as the reaction progressed. The temperature was cooled to 5 °C and held for 7 h. The reaction mixture was filtered on a filter dryer and washed with water (3 × 420 L) to a conductivity specification of <3 mS/cm. The product was dried with an initial nitrogen sweep for about 90 min and then at 50 °C/50 mbar for 18 h. Product **13** was obtained as an off-white solid, 109 kg (96% corrected yield, 95.8 wt %, 100 area % at 220 nm).

***trans*-13a:** ^{1}H NMR (400 MHz, DMSO-d_6) δ 2.09 (s, 3H), 2.35 (s, 3H), 3.34 (s, 3H), 5.93 (broad s, 2H), 6.64 (d, J = 12.0 Hz, 1H), 7.52 (d, J = 12.0 Hz, 1H), 7.82−7.86 (broad m, 2H); ^{13}C NMR (100 MHz, DMSO-d_6) δ 17.0, 22.6, 53.3, 74.3, 108.5, 120.1, 122.2, 142.4, 155.5, 159.3, 162.6.

dx.doi.org/10.1021/op100270u |*Org. Process Res. Dev.* 2011, 15, 343–352

Scheme 10. Optimized synthesis of 2[a]

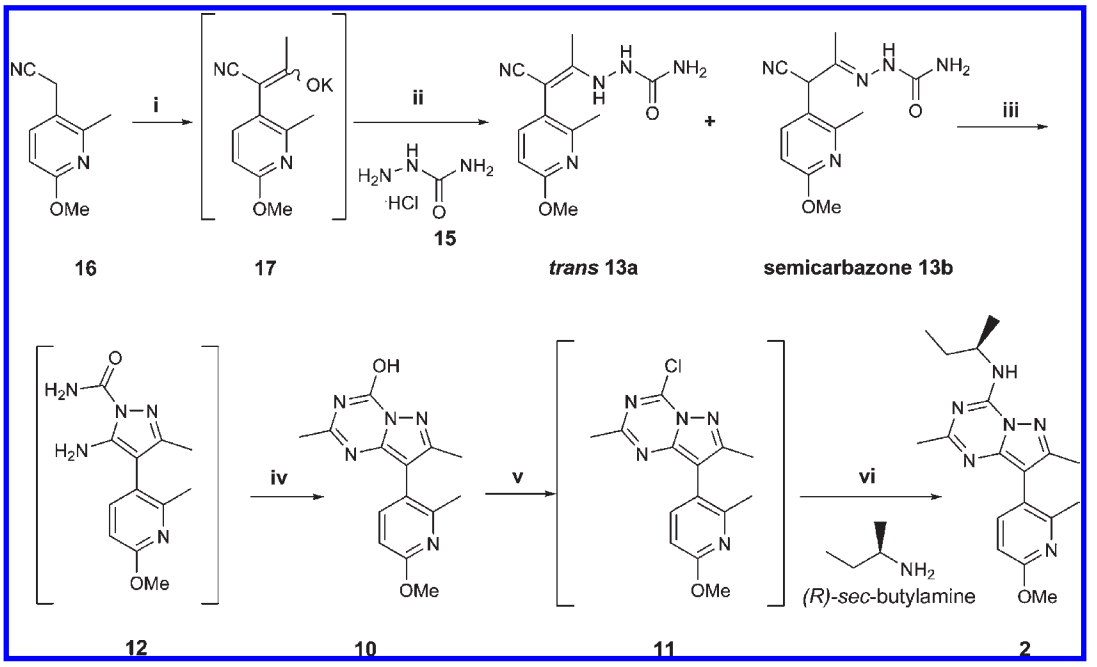

[a] Reagents and conditions: (i) 1.15 equiv of *t*-BuOK in THF, 4.0 equiv of EtOAc, THF; (ii) 2.0 equiv of **15**, H_2O/*i*-PrOH (96%); (iii) 1 mol % DBU, MeCN; (iv) 20 mol % TFA, 1.3 equiv of $H_3CC(OMe)_3$, MeCN (86%); (v) 0.5 mol % *N*-methylmorpholine, 1.3 equiv of $POCl_3$, 2.0 equiv of DIPEA, MeCN; (vi) 1.7 equiv of (*R*)-2-butylamine, 1.0 equiv of DIPEA, MeCN (82%)

Semicarbazone-13b: ^{1}H NMR (400 MHz, DMSO-d_6) δ 1.72 (s, 3H), 2.44 (s, 3H), 3.84 (s, 3H), 5.37 (s, 1H), 6.74 (d, J = 12.0 Hz, 1H), 7.61 (d, J = 12.0 Hz, 1H), 9.54 (s, 1H); ^{13}C NMR (100 MHz, DMSO- d_6) δ 15.5, 23.0, 42.2, 54.2, 109.0, 118.4, 119.9, 140.0, 141.7, 154.7, 157.0, 162.7.

HRMS Calcd for $C_{12}H_{15}N_5O_2$ 261.1226; found 261.1229; Anal. Calcd for $C_{12}H_{15}N_5O_2$: C, 55.16; H, 5.78; N, 26.80. Found: C, 55.03; H, 5.81; N, 26.99.

8-(6-Methoxy-2-methyl-3-pyridyl)-2,7-dimethylpyrazolo-[1,5-α][1,3,5]triazin-4-ol (10). A solution of **13** (650 g, 2.5 mol) in acetonitrile (6.54 L) at 5 °C was treated with a solution of 1,8-diazabicyclo[5.4.0]undec-7-ene (3.75 mL, 24.9 mmol) in acetonitrile (109 mL). The reaction was held for 6 h at which time HPLC analysis indicated >98% conversion to intermediate **12**. Trifluoroacetic acid (37.7 g, 495 mmol) was added followed by the addition of trimethyl orthoacetate (413 mL, 3.24 mol) and a rinse with acetonitrile (435 mL). The jacket temperature was increased to 90 °C over 1 h and held 6 h at which time HPLC analysis indicated >98% conversion to **10**. The temperature was lowered to 60 °C and seeded with **10** (3.16 g, 11.1 mmol). After holding at 60 °C for 1 h, the temperature was lowered over 4 h to 20 °C. A solvent exchange to toluene was accomplished by first removing acetonitrile by distillation at 35 °C and 150 Torr to a volume of 3.25 L. Subsequently, toluene (6.5 L, 62 mol) was charged, and a distillation at 55 °C and 150 Torr served to remove additional acetonitrile. The batch was cooled to 0 °C and aged overnight. The slurry was filtered, washed with toluene (3 × 1.3 L), and dried under vacuum at 50 °C. Product **10** was obtained as a white solid, 616 g (86% corrected yield, 99.9 wt %, 99.9 area % at 220 nm).

^{1}H NMR (400 MHz, $CDCl_3$) δ 2.28 (s, 3H), 2.34 (s, 3H), 2.48 (s, 3H), 3.95 (s, 3H), 6.67 (d, J = 12.0 Hz, 1H), 7.43 (d, J = 12.0 Hz, 1H); ^{13}C NMR (100 MHz, $CDCl_3$) δ 11.2, 19.2, 20.3, 51.7, 105.3, 108.4, 115.5, 139.9, 143.3, 143.8, 151.6, 153.2, 153.8, 160.9; HRMS Calcd for $C_{14}H_{16}N_5O_2$ 286.1304 [M + H]; found 286.1313 [M + H].

4-(2-*R*-Butylamino)-2,7-dimethyl-8-(2-methyl-6-methoxy-3-pyridyl)[1,5-α]-pyrazolo-1,3,5-triazine (2). To a slurry of **10** (42.2 kg, 148 mol) in dry (<1000 ppm) acetonitrile (232 L) was added *N*-methylmorpholine (83 mL, 740 mmol), and *N,N*-diisopropylethylamine (51.5 L, 296 mol). After cooling to 0 °C, phosphorous oxychloride (17.9 L, 192 mol) was added, then the temperature was increased to 25 °C and held until HPLC analysis indicated >98% conversion (1 h). Upon completion of the chlorination reaction, the batch was cooled to −5 °C and MeCN (32 L) was charged. (*R*)-2-Butylamine (25.4 L, 251 mol) was charged over 30 min to maintain the batch temperature <30 °C, followed by *N,N*-diisopropylethylamine (25.8 L, 148 mol). The temperature was increased to 25 °C and after 1 h, HPLC analysis indicated >98% conversion to **2**. The reaction was quenched with water (54.3 L) and 3 N sodium hydroxide (109 L, 325 mol) to a pH <7. The slurry was heated to 65 °C to provide a homogeneous solution, and the reaction mixture filtered through a 10 μm polish filter, followed by an acetonitrile rinse (32 L). The temperature was lowered to 55 °C and water (42 L) was added until a slurry was observed (1 h). Subsequently, the temperature of the batch was lowered to 23 °C, and additional water (295 L) was charged to complete crystallization of the batch. After a 1-h hold, the slurry was transferred to a Hastelloy filter drier with a 10 μm polypropylene cloth, then was washed with 1:1 water/acetonitrile (84 L), followed by water (6 × 170 L) until the conductivity was <30 μS/cm. The product was dried on the filter at 50 °C and 50 mmHg for 16 h, and the product was obtained as a white solid (41.2 kg, 82% corrected yield, 99.2 wt %, 99.8% chiral purity, 99.8 area % at 220 nm).

^{1}H NMR (400 MHz, $CDCl_3$) δ 0.79 (t, J = 12.0 Hz, 3H), 1.11 (d, J = 12.0 Hz, 3H), 1.47 (m, 2H), 2.06 (s, 3H), 2.12 (s, 3H),

dx.doi.org/10.1021/op100270u |*Org. Process Res. Dev.* 2011, 15, 343–352

2.25 (s, 3H), 3.72 (s, 3H), 4.04−4.13 (m, 1H), 6.01 (broad d, J = 12.0 Hz, 1H), 6.41 (d, J = 12.0 Hz, 1H), and 7.19 (d, J = 12.0 Hz, 1H); ^{13}C NMR (100 MHz, $CDCl_3$) δ 10.3, 13.1, 20.4, 22.8, 26.0, 29.6, 48.0, 53.2, 106.5, 107.4, 118.4, 141.5, 146.5, 147.6, 153.6, 155.6, 162.8, 163.7; HRMS Calcd for $C_{18}H_{25}N_6O$ 341.2090 [M + H]; found 341.2088 [M + H]; Anal. Calcd for $C_{18}H_{24}N_6O$: C, 63.5; H, 7.10; N, 24.68. Found: C, 63.49; H, 7.04; N, 24.98.

AUTHOR INFORMATION

Corresponding Author

*E-mail: sevrine.broxer@bms.com

ACKNOWLEDGMENT

We thank our engineering colleagues Otute Akiti, Martina Olzog, Nathan Domagalski, Victor Hung, Brent Nielsen, and Richard Schild for enabling implementation into the pilot plant. We also thank Christopher Wood, John Castoro, Ruben Lozano, Mariann Neverovitch, and Michael Galella for analytical support, and Fucheng Qu for providing the initial observations on the DABCO-catalyzed chlorination. Finally, we acknowledge Lindsay A. Hobson and Rodney L. Parsons, Jr., for helpful discussions, together with PR&D senior management for support during the preparation of the manuscript.

REFERENCES

(1) Vale, W.; Spiess, J.; Rivier, C. *Science* **1981,** *213*, 1394–1397.

(2) For recent reviews, see: (a) Gilligan, P. J. *Expert Opin. Ther. Patents*. **2006,** *16*, 913–924. (b) Arzt, E.; Holsboer, F. *Trends Pharmacol. Sci.* **2006,** *27*, 531–538. (c) Berton, O.; Nestler, E. J. *Neuroscience* **2006,** *7*, 137–151.

(3) Holsboer, F. *Neuropsychopharmacology* **2000,** *23*, 477–501.

(4) (a) Gilligan, P. J.; Clarke, T.; He, L.; Lelas, S.; Li, Y.-W.; Heman, K.; Fitzgerald, L.; Miller, K.; Zhang, G.; Marshall, A.; Krause, C.; McElroy, J. F.; Ward, K.; Zeller, K.; Wong, H.; Bai, S.; Saye, J.; Grossman, S.; Zaczek, R.; Arneric, S. P.; Hartig, P.; Robertson, D.; Trainor, G. *J. Med. Chem.* **2009,** *52*, 3804–3092. (b) Gilligan, P. J.; He, L.; Clarke, T.; Tivitmahaisoon, P.; Lelas, S.; Li, Y.-W.; Heman, K.; Fitzgerald, L.; Miller, K.; Zhang, G.; Marshall, A.; Krause, C.; McElroy, J.; Ward, K.; Shen, H.; Wong, H.; Grossman, S.; Nemeth, G.; Zaczek, R.; Arneric, S. P.; Hartig, P.; Robertson, D. W.; Trainor, G. *J. Med. Chem*. **2009,** *52*, 3073–3083 and references cited therein.

(5) Gilligan, P. J. PCT Int. Appl. WO/2002/072202, 2002.

(6) He, L.; Gilligan, P. J.; Zaczek, R.; Fitzgerald, L. W.; McElroy, J.; Shen, H-S.L.; Saye, J. A.; Kalin, N. H.; Shelton, S.; Christ, D.; Trainor, G.; Hartig, P. *J. Med. Chem*. **2000,** *43*, 449–456.

(7) Gray, M. A.; Konopski, L.; Langlois, Y. *Synth. Commun.* **1994,** *24*, 1367–1379.

(8) Kochetkov, N. K.; Sokolov, S. D.; Vagurtova, N. M. *Zh. Obshch. Khim.* **1961,** *31*, 2326–2333.

(9) Zhou, J.; Oh, L. M.; Ma, P. U.S. Pat. 6,562,965, 2003.

(10) *Hydrazine Hazard Summary*; United States Environmental Protection Agency, (created in April 1992; revised in January 2000; updated in November 2007) 2007; http://www.epa.gov/ttn/atw/hlthef/hydrazin.html (accessed September 9, 2010).

(11) The pyridyl starting material was obtained from commercial sources or by custom synthesis, see: (a) Miyata, H.; Oki, K.; Morikawa, K. JP 2001302658, 2001. (b) Yu, Z. CN 1088574, 1994;(c) Nishida, A.; Shirakawa, S.; Harada, T.; Fujisaki, S.; Kajigaeshi, S. *Technol. Rep. Yamaguchi Univ.* **1988,** *4*, 145–50. (d) Nagel, D. L.; Kupper, R.; Antonson, K.; Wallcave., L . *J. Org. Chem*. **1977,** *42*, 3626–3628. (e) Stogryn, E. L. *J. Org. Chem*. **1972,** *37*, 673. (f) Meyers, A. I.; Collington, E. W. *J. Org. Chem*. **1971,** *36*, 3044–3045. (g) Rapoport, H.; Campion, J. *J. Am. Chem. Soc.* **1951,** *73*, 2239–2241. (h) Page, G. A.; Tarbell, D. S. *J. Am. Chem. Soc.* **1953,** *75*, 2053–2055.

(12) To ensure full dissolution of **16**, 4 equiv were necessary.

(13) Reaction of enolate **17** with semicarbazide **15** in THF/H_2O as solvent did not lead to appreciable levels of conversion.

(14) Pure regioisomers *trans*-**13a** and semicarbazone **13b** were isolated and used for characterization. The *cis*-isomer was not observed.

(15) The isomer ratio was estimated by careful solid-state NMR techniques as **13a** and **13b** were observed to readily interconvert in solution.

(16) Isolation of **10** as a monohydrate required an azeotropic distillation from MeCN to remove H_2O prior to the start of the subsequent API step.

(17) Heating anhydrous **10** to temperatures above 50 °C in the presence of H_2O afforded the monohydrate. Prolonged exposure of anhydrous **10** as a slurry in the presence of water at room temperature did not produce the monohydrate form.

(18) With 1 mol % of DBU, the solubility of **10** is 2 mg/mL whereas with 5 mol % it is 25 mg/mL.

(19) Snodin, D. J. *Regul. Toxicol. Pharmacol*. **2006,** *45*, 79–90.

(20) Anderson, N. G.; Ary, T. D.; Berg, J. L.; Bernot, P. J.; Chan, Y. Y.; Chen, C.-K; Davies, M. L.; DiMarco, J. D.; Dennis, R. D.; Deshpande, R. P.; Do, H. D.; Droghini, R.; Early, W. A.; Gougoutas, J. Z.; Grosso, J. A.; Harris, J. C.; Haas, O. W.; Jass, P. A.; Kim, D. H.; Kodersha, G. A.; Kotnis, A. S.; LaJeunesse, J.; Lust, D. A.; Madding, G. D.; Modi, S. P.; Moniot, J. L.; Nguyen, A.; Palaniswamy, V.; Phillipson, D. W.; Simpson, J. H.; Thoraval, D.; Thurston, D. A.; Tse, K.; Polomski, R. E.; Wedding, D. L.; Winter, W. J. *Org. Process Res. Dev.* **1997,** *1*, 300–310.

(21) Robins, M.; Uznanski, B. *Can. J. Chem*. **1981,** *59*, 2601–2606.

(22) Similar conditions were utilized for a related molecule, see ref 6.

(23) The addition of HCl or LiCl is thought to collapse the intermediate dichlorophosphinate ester, see: (a) Fujino, K.; Takami, H.; Atsumi, T.; Ogasa, T.; Mohri, S.-i; Kasai, M. *Org. Process Res. Dev.* **2001,** *5*, 426–433. (b) Connolly, T. J.; Matchett, M.; Sarma, K. *Org. Process Res. Dev*. **2005,** *9*, 80–87.

(24) Fujino, K.; Takami, H.; Atsumi, T.; Ogasa, T.; Mohri, S.-i.; Kasai, M. *Org. Process Res. Dev*. **2001,** *5*, 426–433.

(25) A similar dimeric impurity has been observed, see ref 20.

(26) The influence of solvent for the chlorination reaction is under investigation and will be reported in due course.

(27) Recently, patents reporting the use of DABCO as catalyst were published, see: (a) Aiqing F. Zhuanli F. Shuomingshu G. S., CN 101423498 A 20090506 (CAN 150:563847 AN 2009:561663), 2009. (b) Aiqing F. Zhuanli F. Shuomingshu G. S. CN 101445485 A 20090603 (CAN 151:78133 AN 2009:689505), 2009.

(28) The exact role of DABCO in the catalyzed chlorination is currently under investigation and will be disclosed in due course.

(29) (a) Robins, R.; Christensen, B. E. *J. Am. Chem. Soc.* **1952,** *74*, 3624–3627. (b) Robins, M.; Uznanski, B. *Can. J. Chem*. **1981,** *59*, 2601–2607. (c) Boyle, P. H.; Gillespie, P. *J. Chem. Res. (S)* **1989,** *9*, 282 also see ref 23.

(30) Doronina, S. O.; Gall, A. A.; Shishkin, G. V. *Khim. Geterotsikl. Soedin.* **1992,** *8*, 1091–1094.

(31) On 40 kg input scale, 30 kg of $POCl_3$ was added in 4 min, resulting in an increase of batch temperature from −4 to 3.5 °C with the jacket temperature set to −10 °C.

(32) Schreiber, S. *Tetrahedron Lett*. **1980,** *21*, 1027–1030.

(33) Enamine formation may occur via hydride transfer as described in ref 32 or as shown below: